Journal of Southeast University (English Edition) Vol. 22, No. 2, pp. 148 – 152 June 2006 ISSN 1003—7985

Low complexity joint source-channel decoding for transmission of wavelet compressed images

Yin Weiwei Mei Zhonghui Wu Lenan

(College of Information Science Engineering, Southeast University, Nanjing 210096, China)

Abstract: To utilize residual redundancy to reduce the error induced by fading channels and decrease the complexity of the field model to describe the probability structure for residual redundancy, a simplified statistical model for residual redundancy and a low complexity joint source-channel decoding (JSCD) algorithm are proposed. The complicated residual redundancy in wavelet compressed images is decomposed into several independent 1-D probability check equations composed of Markov chains and it is regarded as a natural channel code with a structure similar to the low density parity check (LDPC) code. A parallel sum-product (SP) and iterative JSCD algorithm is proposed. Simulation results show that the proposed JSCD algorithm can make full use of residual redundancy in different directions to correct errors and improve the peak signal noise ratio (PSNR) of the reconstructed image and reduce the complexity and delay of JSCD. The performance of JSCD is more robust than the traditional separated encoding system with arithmetic coding in the same data rate.

Key words: joint source-channel decoding; sum-product algorithm; generalized distribution law; wavelet compressed image

In conventional communication systems for data, speech and image etc., correlation in the source is compressed as much as possible and a channel code has to be added to protect digital data from errors induced by noisy channels. This two-step method is supported by Shannon's separation theorem. However this theorem does not hold in practical situations where the power, bandwidth, delay and complexity of the system are limited, because the popular variable-length source coding, such as arithmetic coding is very sensitive to channel errors and a single error blows up the whole scheme. In Ref. [1], it was proposed that some redundancy should be left in the source data so that it could be tolerant of a few transmission errors. The redundancy could be exploited by joint source-channel decoding (JSCD) rather than being extracted by source encoding. JSCD based on residual redundancy can provide a more robust performance for transmission over noisy channels.

The residual redundancy in the encoded source is often regarded as first order or higher order Markov chains (MC)[2-3]. Previous work assumed viewing the combination of an encoded source with redundancy and a noisy channel as a discrete hidden Markov model (HMM) with transmitted indices corresponding to hidden states and received indices corresponding to observables produced within those states[4]. But the practical model of residual redundancy in encoded multimedia source is more complex than the Markov chain.

In order to utilize the complicated residual redundancy in WT compressed image with a lower complexity, we developed a simple yet efficient probability model composed of an independent 1-D probability check equation (PCE) to describe the statistical character and apply a novel JSCD scheme based on SP and an iterative algorithm[5-6].

The contribution of our work is: First, the high-dimensional state transition matrix (STM) can be separated into several 2-D STMs, so the complicated residual redundancy of the WT compressed image is described as some independent PCE in different directions similar to the structure of the LDPC code. Secondly, with this model, we develop a simple and parallel JSCD algorithm based on the SP and iterative algorithm for quantized WT compressed image coefficients corrupted by noise.

Our results indicate that the proposed scheme is robust, simple and efficient for image communication. It provides significant benefits over the previous JSCD of WT compressed image, not only in performance but also in complexity.

1 Probability Model for Wavelet Compressed Images

1.1 Hidden Markov random field (HMRF) model for JSCD of WT coefficients

Wavelet decompositions have proven to be ex-

Received 2005-06-07.

Biographies: Yin Weiwei (1978—), female, graduate; Wu Lenan (corresponding author), male, professor, wuln@seu.edu.cn.

tremely effective for image compression and provide better compression quality than the traditionally used JPEG algorithm. Similar to the Fourier transform, WT is quite good at decorrelating the second order statistics of natural signals. However, the WT cannot completely decorrelate real-world signals and images—a residual dependency structure always remains between the wavelet coefficients. In WT domain of images, there are 2-D spatial or more complicated dependencies among quantized wavelet image coefficients which are to be transmitted over noisy channels. MC fails to capture this a priori knowledge. The dependency within subband is usually modeled as the Markov random field (MRF) and dependencies across the scales can be modeled as the Markov tree. In order to keep robustness in communication over noisy channels, these redundancies can not be removed by entropy coding. So the quantized WT coefficients with field correlation over noisy channels can be regarded as HMRF in JSCD. But the prohibitive complexity of the HMRF model limited in its application. A simplified hidden Markov mesh random field (HMMRF) is addressed in Ref. [4]. But only the neighbor states in horizontal and vertical directions are considered in HMMRF and the dependencies in the field cannot be represented perfectly. Furthermore, the state transition probability matrix of HMMRF is still a complicated 3-D matrix composed of $P(S_{k,l}/S_{k-1,l}, S_{k,l-1})$, where k, l are the position indices of the state S. If the dependencies in all directions of the integrated field are considered, the state transition probability matrix will be 5-D and becomes computationally intractable.

1.2 Probability field model composed of 1-D PCE for WT coefficients

The correlation of field within wavelet subband exists in four directions, and there are eight neighbors around one state. That is to say, every state to be decoded is constrained by its eight neighbors in a probability sense (see Fig. 1). We can represent it using the Tanner graph (see Fig. 2) which is often used in decoding of LDPC. Every edge in the Tanner graph represents a local check equation. Fig. 2 is only a part of the Tanner graph of all WT coefficients.

Algorithms that deal with complicated global functions of many variables, such as the SP, often exploit the manner in which the given functions are factorized into a product of "local" functions, each of which depends on a subset of the variables. But the SP algorithm is used in the cycle-free case theoretically. We can apply it in the case of cycles by the following iterative algorithm[5]. A message from a function node

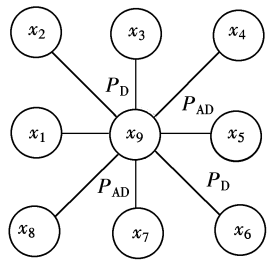

Fig. 1 Departmency structure of coefficients within WT subband

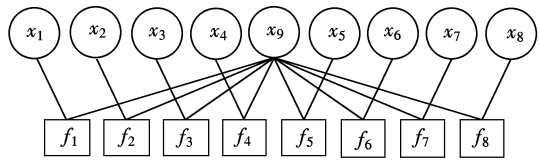

Fig. 2 Tanner graph of WT coefficients

to a variable node is the marginalization of the product of all the messages incoming to the function node and the function itself.

In the Tanner graph of LDPC, one bit is constrained by several independent check equations. If we can separate the field model into independent separated 1-D local check equations, the statistical dependencies in the field are regarded as the natural channel code which possesses the structure similar to LDPC. The SP and iterative algorithm used in LDPC decoding can be adopted to decode source symbols with redundancy to combat channel noise.

2 JSCD Using Sum-Product Algorithm

Assume that f_i is a local function which depends on x_9 and its neighbour state x_i is shown in Fig. 1. S_i is the event that satisfies check equation f_i. If and only if $S_1, S_2, \ldots, S_8$ is statistically independent, we have

$$P(S_1, S_2, \ldots, S_8, x_9/\{y\}) = \prod_{i=1}^{8} P(S_i/x_9, \{y\}) P(x_9/\{y\}) \tag{1}$$

That is to say, the posterior probability can be computed as the product of eight factors. We are interested in developing the probability model composed of eight independent functions which represent the dependencies in different directions.

From Fig. 1, we obtain

$$P(x_9/x_2) = \sum_{x_1, x_3} P(x_9, x_1, x_3/x_2) = \sum_{x_1, x_3} P(x_1, x_3/x_2) P(x_9/x_1, x_2, x_3) \tag{2}$$

Assume that $P(x_9/x_1, x_2, x_3)$ can be factorized into $P(x_9/x_1, x_3)$ and $P_D(x_9/x_2)$. The first term represents the dependency between x_9 and the local domain $\{x_1, x_3\}$, and the second represents the dependency between x_9 and x_2, i. e. ,

$$P(x_9/x_2) = \sum_{x_1, x_3} P(x_1, x_3/x_2) P(x_9/x_1, x_2, x_3) = \sum_{x_1, x_3} P(x_1, x_3/x_2) P(x_9/x_1, x_3) P_{\mathrm{D}}(x_9/x_2) \quad (3)$$

For the given statistical probabilities $P(x_9/x_2)$, $P(x_1, x_3/x_2)$ and $P(x_9/x_1, x_3)$, the independent probability check equation in diagonal direction is given by

$$P_{\mathrm{D}}(x_9/x_2) = \frac{P(x_9/x_2)}{\sum_{x_1, x_3} P(x_1, x_3/x_2) P(x_9/x_1, x_3)} \quad (4)$$

So we have

$$\sum_{x_1, x_2, x_3} P(x_9/x_1, x_2, x_3) = \sum_{x_1, x_2, x_3} P(x_9/x_1, x_3) P_{\mathrm{D}}(x_9/x_2) = \sum_{x_1, x_3} P(x_9/x_1, x_3) \sum_{x_2} P_{\mathrm{D}}(x_9/x_2) \quad (5)$$

According to the above equations, we obtain an independent PCE of $P_{\mathrm{D}}(x_9/x_2)$ which represents statistical dependency between two neighbor states in diagonal direction. The PCE of $P_{\mathrm{AD}}(x_9/x_4)$ in anti-diagonal direction is obtained in the same way. Because x_2 is independent of $\{x_5, x_6, \ldots, x_9\}$, we can obtain

$$\sum_{x_1, x_2, \ldots, x_8} P(x_9/x_1, x_2, \ldots, x_8) = \sum_{x_1, x_3, \ldots, x_8} P(x_9/x_1, x_3, \ldots, x_8) \sum_{x_2} P_{\mathrm{D}}(x_9/x_2) \quad (6)$$

Likewise, we can factorize $P(x_9/x_1, x_2, \ldots, x_8)$ into the dependencies in different directions,

$$\sum_{x_1, x_2, \ldots, x_8} P(x_9/x_1, x_2, \ldots, x_8) = \sum_{x_1, x_3, x_5, x_7} P(x_9/x_1, x_3, x_5, x_7) \sum_{x_2} P_{\mathrm{D}}(x_9/x_2) \cdot \sum_{x_4} P_{\mathrm{D}}(x_9/x_4) \sum_{x_6} P_{\mathrm{D}}(x_9/x_6) \sum_{x_8} P_{\mathrm{D}}(x_9/x_8) \quad (7)$$

The posterior probability of the decoded state x_9 can be expressed as

$$P(x_9/y_1, y_2, \ldots, y_9) \propto P(y_1, y_2, \ldots, y_9/x_9) P(x_9) = P(y_1, y_2, \ldots, y_8/x_9) P(y_9/x_9) P(x_9) \propto P(x_9/y_1, y_2, \ldots, y_8) P(y_9/x_9) = \sum_{x_1, x_2, \ldots, x_8} P(x_9/x_1, x_2, \ldots, x_8) \cdot P(x_1, x_2, \ldots, x_8/y_1, y_2, \ldots, y_8) P(y_9/x_9) = \sum_{x_1, x_2, \ldots, x_8} \frac{P(x_1, x_3, x_5, x_7/x_9) P(x_9)}{P(x_1, x_3, x_5, x_7)} \cdot P_{\mathrm{D}}(x_9/x_2) P_{\mathrm{AD}}(x_9/x_4) P_{\mathrm{D}}(x_9/x_6) P_{\mathrm{AD}}(x_9/x_8) \cdot P(x_1, x_2, \ldots, x_8/y_1, y_2, \ldots, y_8) P(y_9/x_9) \quad (8)$$

To reduce the complexity of the model, we made the assumption that the neighbor states in the horizontal and vertical directions are statistically independent given the current state, i. e. ,

$$P(x_1, x_3, x_5, x_7/x_9) = P(x_1/x_9) P(x_3/x_9) P(x_5/x_9) P(x_7/x_9) \quad (9)$$

Hence, Eq. (8) can be rewritten as

$$\sum_{x_1, x_2, \ldots, x_8} \frac{P(x_9/x_1) P(x_9/x_3) P(x_9/x_5) P(x_9/x_7)}{P(x_1, x_3, x_5, x_7) P(x_9) P(x_9) P(x_9)} \cdot \frac{P(x_1) P(x_3) P(x_5) P(x_7)}{P(x_1, x_3, x_5, x_7) P(x_9) P(x_9) P(x_9)} P_{\mathrm{D}}(x_9/x_2) \cdot P_{\mathrm{AD}}(x_9/x_4) P_{\mathrm{D}}(x_9/x_6) P_{\mathrm{AD}}(x_9/x_8) \cdot P(x_1, x_2, \ldots, x_8/y_1, y_2, \ldots, y_8) P(y_9/x_9) \quad (10)$$

The joint posterior probability distribution of states $\{x_1, x_2, \ldots, x_8\}$ can be approached by the product of state posterior probability updated by the iterative algorithm, so we have

$$\frac{P(x_1) P(x_3) P(x_5) P(x_7)}{P(x_1, x_3, x_5, x_7)} P(x_1, x_2, \ldots, x_8/y_1, y_2, \ldots, y_8) \approx P(x_1/y_1, y_2, \ldots, y_8) P(x_2/y_1, y_2, \ldots, y_8) \ldots P(x_8/y_1, y_2, \ldots, y_8) \quad (11)$$

Because variables $x_1, x_2 \ldots, x_9$ are separated in formula (10), we can use the distributive law to simplify the summations[7]. The posterior probability of x_9 can be computed as

$$\prod_{i=1, 3, 5, 7} \sum_{x_i} \frac{P(x_9/x_i)}{P(x_9)} P(x_i/y_1, y_2, \ldots, y_8) \cdot \prod_{j=2, 6} \sum_{x_j} P_{\mathrm{D}}(x_9/x_j) P(x_j/y_1, y_2, \ldots, y_8) \cdot \prod_{k=4, 8} \sum_{x_j} P_{\mathrm{AD}}(x_9/x_k) P(x_k/y_1, y_2, \ldots, y_8) \cdot \sum_{x_9} P(y_9/x_9) P(x_9) \quad (12)$$

where $y_1, y_2, \ldots, y_9$ are the observations of $x_1, x_2, \ldots, x_9$ corrupted by the noisy channel. $P(x_9)$ is the a priori probability of quantized index x_9. $P(y_1/x_1)$ is the likelihood function. If we use f_i to represent the local check equation of x_i and x_9, Eq. (12) is denoted by $\prod_{i=1}^{9} f_i$.

3 JSCD Using Markov Tree Dependency between Subbands in Different Scales

Wavelet-based image compression enables multiresolution progressive reconstruction of the image at the receiver. For the image transmission, progressive image codec have been shown to be very useful because they can produce an increasing quality reconstruction of the original image at the receiver using a minimum amount of the channel capacity. Large/small values of WT coefficients tend to propagate through the scales of the quad-trees (see Fig. 3)[8]. The inter-scale dependency of HL, LH and HH subbands can be captured by the Markov tree model. When WT coefficients of more than one scale are received, our JSCD scheme can incorporate both inter-scale dependency and intra-scale dependency simultaneously without increasing too much complexity.

Considered the inter-scale dependency, x_9 is con-

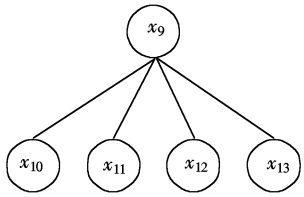

Fig. 3 Quad-tree organization of the wavelet coefficient in one subband of the wavelet transform

strained by x_{10} to x_{13} besides x_2 to x_9. Using the algorithm mentioned above, we have

$$P(x_9/y_1, y_2, \ldots, y_{13}) = \prod_{i=1}^{13} f_i \qquad (13)$$

where $f_1, f_2, \ldots, f_9$ are defined as mentioned above, and $f_{10}, f_{11}, f_{12}, f_{13}$ are computed as

$$f_{10} = \sum_{x_{10}} P_1(x_9/x_{10}) P(x_{10}/y_{10}, y_{11}, \ldots, y_{13})$$

$$f_{11} = \sum_{x_{11}} P_2(x_9/x_{11}) P(x_{11}/y_{10}, y_{11}, \ldots, y_{13})$$

$$f_{12} = \sum_{x_{12}} P_3(x_9/x_{12}) P(x_{12}/y_{10}, y_{11}, \ldots, y_{13})$$

$$f_{13} = \sum_{x_{13}} P(x_9/x_{13}) P(x_{13}/y_{10}, y_{11}, \ldots, y_{13})$$

Given the probabilities from training data, $P_1(x_9/x_{10})$, $P_2(x_9/x_{11})$ and $P_3(x_9/x_{12})$ are computed as

$$P_1(x_9/x_{10}) = \frac{P(x_9/x_{10})}{\sum_{x_{11}, x_{12}, x_{13}} P(x_9/x_{11}, x_{12}, x_{13}) P(x_{11}, x_{12}, x_{13}/x_{10})}$$

$$P_2(x_9/x_{11}) = \frac{P(x_9/x_{11})}{\sum_{x_{12}, x_{13}} P(x_9/x_{12}, x_{13}) P(x_{12}, x_{13}/x_{11})}$$

$$P_3(x_9/x_{12}) = \frac{P(x_9/x_{12})}{\sum_{x_{13}} P(x_9/x_{13}) P(x_{13}/x_{12})}$$

The complexity of HMRF is in the order of N^5T, which is considered significantly high, where N is the number of the states in the model and T is the total number of the states in the encoded image source. The complexity of HMMRF is reduced to N^3T, and the proposed scheme using the sum-product algorithm is N^2T only.

4 Simulation Results

Fig. 4 depicts reconstructions of the WT compressed 512 × 512 Lenna image with various decoders over a flat Rayleigh fading channel. The statistics needed are obtained using ten images, which exclude the test image Lenna. In Figs. 4(a) to (d), only the subband of one scale is received and the intra-scale field dependency is exploited in JSCD. The coefficients are 4-bit Lloyd-max quantized at 0.25 bit/pixel. In Figs. 4(e) to (h), the subbands of two scales are received, both inter-scale and intra-scale dependencies are utilized with the sum-product JSCD. 2-bit quantization is used and results in a 0.5 bit/pixel compression.

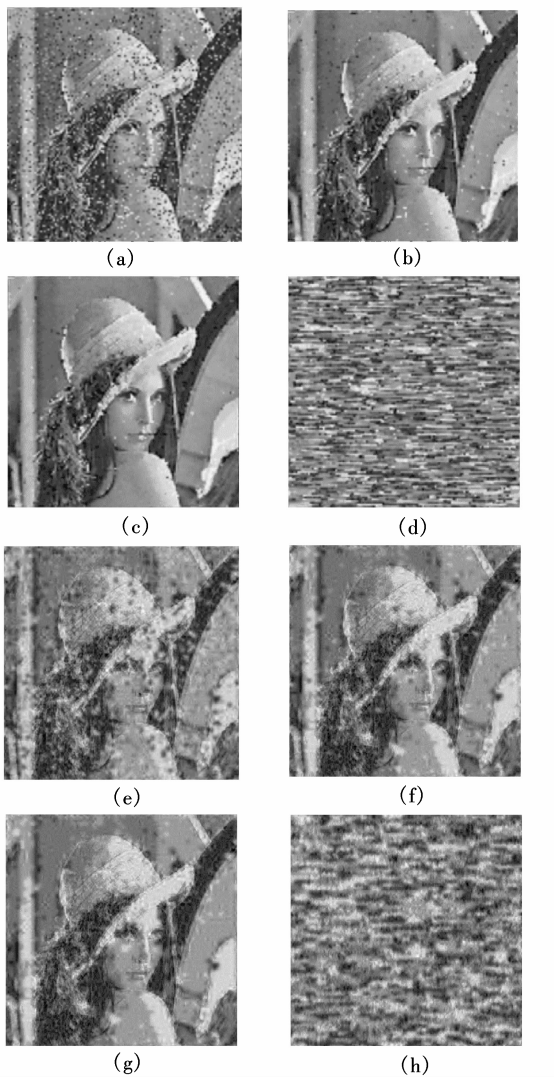

Fig. 4 "Lenna" reconstructed with different schemes, $E_b/N_0 = 3$ dB. (a) Standard, 19.96 dB; (b) HMMRF, 23.35 dB; (c) The SP JSCD, 24.04 dB; (d) Arith_LDPC, 12.13 dB; (e) Standard, 18.90 dB; (f) HMMRF, 20.42 dB; (g) The SP JSCD, 20.85 dB; (h) Arith_LDPC, 12.10 dB

Fig. 5 compares PSNR vs. channel SNR curves for various schemes. JSCD using the SP algorithm and the HMMRF model outperforms the standard decoder by about 2 to 4 dB. In comparison with HMMRF, we find our SP algorithm obtained better performance with lower complexity. Because the degree of the symbol to be decoded in the Tanner graph is high, so the number of iterations is small and two iterations are enough in our simulation.

The Arith_LDPC system uses arithmetic coded WT coefficients with LDPC code protection at the same data rate as the JSCD scheme. Due to the error propagation of the entropy code, it is not suitable for noisy channels.

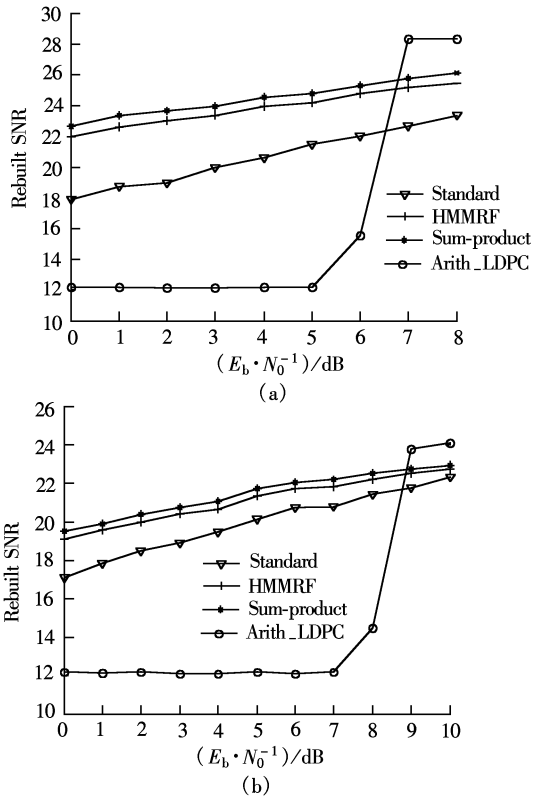

Fig. 5 Comparison of several schemes for transmission of WT compressed images over noisy channels. (a) Only one scale subband is received; (b) Subbands of two scales are received

5 Conclusion

We have studied a novel JSCD algorithm for transmission of WT compressed images over a flat Rayleigh fading channel. Simulations indicate that the proposed JSCD scheme achieves a better quality of the WT compressed image with lower complexity than other JSCD techniques in the previous literature. In contrast to the traditional Tandem system of entropy code and LDPC protection at the same data rate, it is more robust and efficient when transmitting over a noisy and fading channel.

References

[1] Buch G, Burkert F, Hagenauer J, et al. To compress or not to compress [A]. In: *Proc of IEEE Communications Theory Miniconf* [C]. London, 1996. 198 – 203.

[2] Fingscheidt T, Hindelang T, Cox R V, et al. Joint source-channel (de-) coding for mobile communications[J]. *IEEE Trans Commun*, 2002, **50**(2): 200 – 212.

[3] Lahouti F, Khandani A K. Efficient source decoding over memoryless noisy channels using higher order Markov models [J]. *IEEE Transactions on Information Theory*, 2004, **50**(9): 2103 – 2118.

[4] Park M, Miller D J. Improved image decoding over noisy channels using minimum mean-squared estimation and a Markov mesh [J]. *IEEE Transactions on Image Process*, 1999, **8**(6): 863 – 867.

[5] Kschischang F R, Frey B J, Loeliger H A. Factor graphs and the sum-product algorithm [J]. *IEEE Transactions on Information Theory*, 2001, **47**(2): 498 – 519.

[6] Kschischang F R, Frey B J. Iterative decoding of compound codes by probability propagation in graphical models [J]. *IEEE Journal on Selected Areas in Communications*, 1998, **16**(2): 219 – 230.

[7] Aji S M, McEliece R J. The generalized distributive law [J]. *IEEE Transactions on Information Theory*, 2000, **46**(2): 325 – 343.

[8] Romberg J K, Hyeokho Choi, Baraniuk R G. Bayesian tree-structured image modeling using wavelet-domain hidden Markov models [J]. *IEEE Transactions on Image Process*, 2001, **10**(7): 1056 – 1068.

小波压缩图像传输的低复杂度信源–信道联合译码

殷玮玮　梅中辉　吴乐南

(东南大学信息科学与工程学院, 南京 210096)

摘要: 为了利用小波压缩图像的残留冗余减小其经过衰落信道造成的传输错误,并针对直接利用场模型描述残留冗余概率结构带来的较高计算复杂度,提出了一种简化的残留冗余统计模型和低复杂度的信源–信道联合译码方法. 小波压缩图像的复杂残留冗余统计模型被简化成多个独立的一维 Markov 链构成的统计校验方程,并被看作是一种具有类似于 LDPC 码结构的天然信道编码,在此基础上设计出一种并行的和积迭代联合译码算法. 仿真显示该联合译码算法既可以充分利用多个方向的残留冗余进行纠错,提高重建图像的 PSNR,又可以减小联合译码的复杂度和延时,并且在同样的数据传输率下,比利用算术码的传统分离编码系统鲁棒性更好.

关键词: 信源–信道联合译码;和积算法;广义分配率;小波压缩图像

中图分类号: TN91